J. theor. Biol. (1980) **86,** 455–475

Unstable Dynamics of a Periodically Driven Oscillator in the Presence of Noise

LEON GLASS, CARL GRAVES, GINO A. PETRILLO AND MICHAEL C. MACKEY

Department of Physiology, McIntyre Medical Building, McGill University, 3655 Drummond Street, Montreal, Quebec, Canada H3G 1Y6

(*Received* 1 *October* 1979, *and in revised form* 14 *February* 1980)

Two qualitatively different unstable dynamical behaviours are shown to arise from the application of a periodic input to a simple mathematical model of an oscillator in the presence of noise. Rhythms similar to quasiperiodic dynamics may arise when there is a low amplitude periodic input, while with high amplitude inputs, patterns with irregular skipped or intercalated beats are found. These two qualitatively different types of unstable dynamics are similar to those observed in the respiratory activity of mechanically ventilated cats. A number of numerical simulations are performed to illustrate the quantitative properties of the two unstable patterns and to show how the quantitative properties can be compared with experimental data.

1. Introduction

Often a biological rhythm in an organism may be affected by other rhythms in the same organism or by external rhythms imposed from the outside. Interaction between the rhythms may lead to entrainment or phase locking, so that for every N cycles of one rhythm there are M cycles of the second rhythm, where N and M are (typically small) integers. Moreover, the two rhythms may phase lock with fixed phase relations. Representative examples of phase locking include: synchronization of circadian activity cycles to light–dark cycles of 24 hours (Bunning, 1967; Swade, 1969; Pavlidis, 1973); synchronization of limbs during locomotion (Van Holst, 1973; Stein, 1976, 1978); synchronization of the heart beat to periodic stimulation (Moulopoulos, Kardaras & Sideris, 1965; Reid, 1969; van der Tweel, Meijler & van Capelle, 1973), synchronization of pacemaker neurons in sea slugs to periodic stimulation of inhibitory interneurons (Moore, Segundo & Perkel, 1963; Perkel *et al.*, 1964; Pinsker, 1977), and synchronization of glycolysis to periodic addition of substrate (Boiteux, Goldbeter & Hess, 1975).

0022-5193/80/190445+21 $02.00/0

In preparations in which phase locking has been found, there are sometimes circumstances in which phase locking does not occur and the resulting rhythms are not periodic in time (Ayers & Selverston, 1979; Boiteux, Goldbeter & Hess, 1975; Moulopoulos, Kardaras & Sideris, 1965; Pavlidis, 1973; Perkel *et al.*, 1964; Pilkington, 1976; Reid, 1969; Swade, 1969; van der Tweel, Meijler & van Capelle, 1973; von Holst, 1973; Wendler, 1974; Wilkens & Young, 1975). These rhythms have been called "oscillatory free runs" in the circadian literature (Swade, 1969; Pavlidis, 1973), and are often referred to as a type of "relative co-ordination" in the neural oscillator literature (von Holst, 1973; Ayers & Selverston, 1979). A related phenomenon, the periodic respiratory modulation of cardiac frequency is called "respiratory sinus arrhythmia" (Watanabe & Dreifus, 1977). Most theoretical and experimental work has concentrated on the analysis of stable phase locked patterns, and relatively little attention has been given to the mechanisms underlying the generation of unstable patterns of oscillator interactions (see, however, Moore, Segundo & Perkel, 1963; Swade, 1969; Pavlidis, 1973). Here, a unified, simple mechanism for the generation of phase locking phenomenon and unstable patterns from the interaction of biological oscillators is described.

Our interest in these unstable patterns has been stimulated by experimental work, currently under way in our laboratory, examining the phase locking of the phrenic nerve activity of a paralyzed, anesthetized cat to a ventilator. The phrenic nerve innervates the diaphragm and phrenic nerve activity causes the diaphragm to contract and descend, promoting inspiration. In the paralyzed cat, the neuromuscular junctions at the diaphragm are blocked and phrenic activity does not cause inspiration. However, lung inflation nevertheless serves to modulate the respiratory rhythm generated in the brainstem by the Hering–Breuer reflexes (Clark & von Euler, 1972; Wyman, 1977). These reflexes shorten inspiratory time (the interval during which the phrenic nerve is active) and lengthen expiratory time (the interval during which the phrenic nerve is silent) during lung inflation. By changing the frequency and amplitude of the ventilator, a variety of different phase locking patterns (e.g. ventilator frequency/phrenic frequency = 1/2, 2/3, 1/1, 3/2, 2/1, 3/1) can be elicited (Petrillo, Glass & Trippenbach, 1980). In addition to these phase locked patterns, there are also patterns which are not phase locked. Two typical examples taken from recordings of about 50 ventilation periods are shown in Fig. 1.

In Fig. 1(a) there is a continuous phase shift of the phrenic activity so each subsequent phrenic onset occurs later in the ventilation cycle. This is similar to "oscillatory free runs" (Swade, 1969; Pavlidis, 1973), to unstable patterns often observed in coupled neural oscillators (Ayers & Selverston,

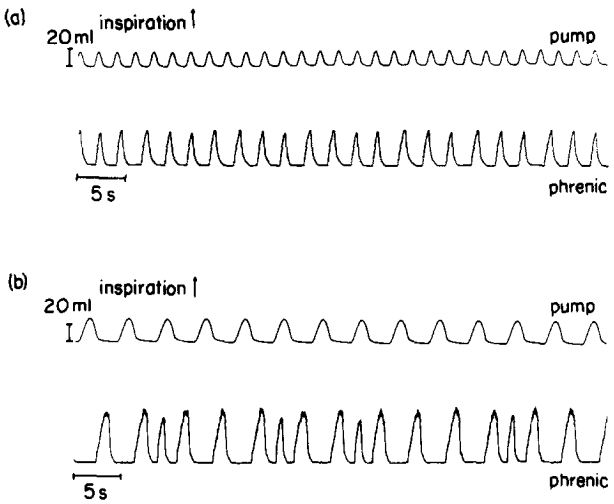

FIG. 1. Examples of non-phase locked respiratory behaviour in anesthetized, paralyzed, artificially ventilated cats. Records (a) and (b) are from different animals. (a) "Quasi-periodic" behaviour showing a progressive phase shift between pump cycle and phrenic activity. Pump frequency = 30 min^{-1}, inflation volume = 18 ml, end-tidal CO_2 = 6·0%, end tidal O_2 = 15%. (b) Asynchronous behaviour between pump cycle and phrenic activity. Pump frequency = 14·3 min^{-1}, inflation volume = 30 ml, end-tidal CO_2 = 6·8%, end tidal O_2 = 16%.

1979; Pilkington, 1976; von Holst, 1973; Wendler, 1974; Wilkens & Yound, 1975) and to unstable patterns observed from periodic input to the heart (Moulopoulos, Kardaras & Sideris, 1965; Reid, 1969; van der Tweel, Meijler & van Capelle, 1973).

The pattern in Fig. 1(b) is quite different from 1(a). During some ventilator cycles there is one phrenic burst and during others there are two. However, we have not found a way to predict whether one or two phrenic bursts will occur in any given ventilator cycle. Although patterns similar to Fig. 1(b) have not, to our knowledge, been previously described in the experimental literature, some cardiac arrhythmias display skipped (or extra, or different) beats occurring at unpredictable intervals (Brooks & Lu, 1973; Pick, Langendorf & Jedlicka, 1973; Watanabe & Dreifus, 1977).

A major motivation for this work is the observation that the two types of experimentally observed dynamics displayed in Fig. 1 appear to be related to two possible types of unstable dynamics in a deterministic model for phase locking which has recently been proposed (Glass & Mackey, 1979). In this model, described in section 2, long and complex phase locking patterns were observed. In section 3, we show by computer simulation that the addition of noise to the deterministic model destroys these complex phase locking

patterns. Moreover, there is a striking qualitative similarity between the patterns in the mathematical model and the experimentally observed unstable coupling patterns (cf. Fig. 1 and Fig. 2). In section 4 the implications of this work for experimental biologists, mathematicians, and clinicians are discussed. The Appendix contains an algorithm for computing phase locking patterns for the model in the absence of noise.

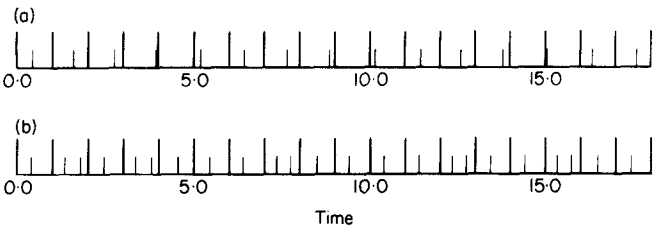

FIG. 2. Representative examples showing unstable coupling patterns for the model described in section 3. The long, heavy bars mark successive periods of the periodic sinusoidal input, whereas the short, lighter bars mark the firing times of the model oscillator with 5% noise. The qualitative behaviour corresponds closely to the experimentally observed coupling patterns shown in Fig. 1. The parameters (see sections 2 and 3 for definition) are: (a) $k = 0{\cdot}05$, $\lambda^{-1} = 1{\cdot}23$; and (b) $k = 0{\cdot}4$, $\lambda^{-1} = 0{\cdot}72$.

2. A Simple Model for Phase Locking (Glass & Mackey, 1979)

In the respiratory system, lung inflation shortens inspiratory time. The precise mechanism underlying this phenomenon is not fully understood. However, there is evidence that activity from stretch receptors in the lungs (carried through vagal fibres), summates with activity from inspiratory neurons in the brain stem. When the summated activity reaches a certain critical value, the "off-switch threshold" inspiration is terminated (Bradley *et al.*, 1975; Cohen & Feldman, 1977). From a mathematical perspective, this mechanism is equivalent to a periodic modulation of a fixed threshold by lung inflation.

In our model for phase locking we have considered the effects of sinusoidal modulation of the threshold for the simple "integrate and fire" model. Although this model was motivated by a consideration of the respiratory control system, it is not completely suitable to describe control of respiration since the timing of expiration has been neglected. However, as shown below there are striking similarities between the dynamics of the simple model and phase locking in the respiratory system.

Assume that an activity $X(T)$ is zero at $T = T_0$ and increases linearly at a rate Λ,

$$X(T) = \Lambda(T - T_0), \tag{1}$$

until it reaches a threshold, $\Theta(T)$

$$\Theta(T) = \Theta_0 + K \sin \omega T, \qquad 0 \leq K < \Theta_0, \tag{2}$$

where Θ_0 is the mean value of the threshold, K is the amplitude of the perturbation and ω is the angular frequency of the perturbation. On reaching threshold, the activity resets to zero, and immediately starts increasing linearly until it again reaches threshold, and so forth.

The model equations can be rewritten in terms of dimensionless variables. Set

$$\begin{aligned} t &= \omega T/2\pi \\ x(t) &= X(T)/\Theta_0 \\ \theta(t) &= \Theta(T)/\Theta_0 \\ k &= K/\Theta_0 \\ \lambda &= 2\pi\Lambda/\omega\Theta_0 \end{aligned} \tag{3}$$

so (1) and (2) become

$$x(t) = \lambda(t - t_0) \tag{4}$$

$$\theta(t) = 1 + k \sin 2\pi t, \qquad 0 < k < 1. \tag{5}$$

Note that in (4) and (5), as in (1) and (2), the ratio of the frequency of the sinusoidal threshold modulation to the frequency of the autonomous oscillator ($K = k = 0$) is λ^{-1}.

The properties of the model for phase locking can be numerically determined by solving (4) and (5) for the minimal root $t_1 > t_0$, where t_1 represents the first firing time (the time when the activity reaches threshold for the first time). In a similar fashion the nth firing time (t_n) can be determined by solving

$$x(t) = \lambda(t - t_{n-1}) \tag{6}$$

and (5) for the minimal root $t_n > t_{n-1}$. This thus defines an algorithm for determining the sequence of firing times, $t_1, t_2, \ldots, t_n$, which can also be represented by a function g, given by

$$t_{n+1} = g(t_n). \tag{7}$$

We will also write

$$t_{n+1} (\text{mod } 1) = G(t_n) = g(t_n) (\text{mod } 1). \tag{8}$$

Since the threshold curve is periodic with period 1, phase locking will occur if

$$\lim_{n \to \infty} [t_{n+M} (\text{mod } 1) - t_n (\text{mod } 1)] = 0. \tag{9}$$

If (9) is satisfied we say that there is N/M phase locking where N is the integer defined by

$$N = \lim_{n \to \infty} (t_{n+M} - t_n) \tag{10}$$

and M is the smallest integer for which (9) is satisfied.

Numerical and analytical methods have been used to study the regions of N/M phase locking and the stability of the coupling patterns (Glass & Mackey, 1979; Keener, Hoppensteadt & Rinzel, 1980). The results of these computations are summarized in Fig. 3, which shows the principal phase locking regions. In addition to the regions indicated, other regions of higher periodicity are found. Thus in the regions intermediate to the 1/1 and 2/3 regions there are a variety of other patterns, including 6/7, 13/16, 3/4, 5/7, and 7/10, and indeed there are an infinite number of stable phase locking patterns in regions of (λ, k) parameter space between any two stable phase-locking patterns (Glass & Mackey, 1979; Keener, 1980). Numerical studies indicate that the firing patterns in the stable phase locked zones are independent of the initial conditions.

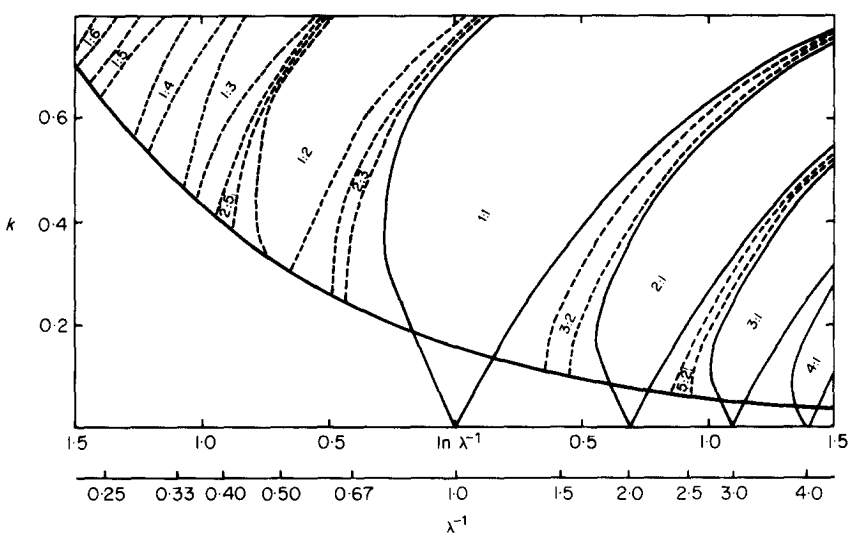

FIG. 3. Phase locking patterns in (λ, k) parameter space for the deterministic system of section 2. The heavy horizontal line separates region A (beneath the line) from region B (above the line). The borders of $N/1$ locking patterns (analytically computed) are indicated by thin solid lines. Other N/M locking patterns, computed numerically, are shown by dashed lines. All phase locked regions extend to $k = 0$. Reproduced with slight modification from Glass & Mackey (1979) with permission.

In addition to these stable phase locked patterns, there are also patterns which are not phase locked. There are two such qualitatively different types of behaviour which occur in different regions of (λ, k) parameter space separated by the heavy horizontal line $(\lambda = 2\pi k)$ in Fig. 3. Region A (below the line) in which $\lambda > 2\pi k$ and region B (above the line) in which $\lambda < 2\pi k$ are discussed below.

In region A the unstable patterns are called quasi-periodic†. For quasi-periodic dynamics the map $G(t_n)$, in equation (8), is topologically equivalent to the map

$$G(t_n) = t_n + \rho (\text{mod } 1), \tag{11}$$

where ρ is an irrational number. If the sequence of points $t_1, t_2, \ldots, t_n$ (mod 1) is mapped to the unit circle, then in the limit $n \to \infty$, the unit circle will be densely covered with points in the sequence (Coddington & Levinson, 1955). Quasi-periodic dynamics in region A are expected to occur on a set of positive measure (Herman, 1977), so a randomly chosen point in (λ, k) parameter space has a finite probability of being quasi-periodic. Quasi-periodic dynamics in the simple model occurs for weak coupling (k small) between the autonomous oscillator and the threshold perturbation.

The unstable dynamics found in region B are of a different type, and have only recently been analytically described (Keener, 1980). In contrast to the quasi-periodic case, if the sequence of times defined by (8) is mapped to the unit circle, the resulting (Cantor) set is nowhere dense on the unit circle (Keener, 1980). The set of (λ, k) in region B for which unstable dynamics occur is of measure zero, which means that a randomly chosen point (λ, k) has zero probability of being in the set of parameter values leading to unstable dynamics. Consequently, if a physical or biological system could be described by the simple model (or one topologically equivalent), unstable patterns should not be seen in the strong coupling regions of parameter space corresponding to region B, Fig. 3.

However, in our experimental studies unstable coupling patterns, not of a quasi-periodic nature [Fig. 1(b)], have been observed. In the next section, the addition of noise to the simple model is demonstrated to give unstable patterns qualitatively similar to that observed in Fig. 1(b).

† The term *ergodic* may be used to characterize the dynamics in this case (Coddington & Levinson, 1955). However, the term quasi-periodic (Moser, 1973) seems preferable since it is more descriptive of the particular sort of ergodic dynamics found. An example of quasi-periodic dynamics is a sine wave whose amplitude is sinusoidally modulated where the ratio of the frequencies of the two sine waves is irrational. It would be inappropriate to call such dynamics "chaotic".

3. The Effects of Noise

In any physical system there are small stochastic fluctuations due to thermal noise. In oscillating biological systems, stochastic fluctuations in period and amplitude are expected due to fluctuations in inputs to the oscillating system. For example, in "integrate and fire" models a more realistic model would be a fluctuating biased random walk towards a fixed or perhaps fluctuating threshold (Moore, Segundo & Perkel, 1963). In the computations which follow, noise is incorporated in a straightforward way suggested to us by A. Lasota.

Assume that to the deterministic equation (7) is added a stochastic perturbation ξ_n, so

$$t_{n+1} = g(t_n) + \xi_n, \tag{12}$$

where ξ_n is uniformly distributed on an interval $\pm\nu$. Here, the noise will be expressed as a percentage, e.g. 5% noise for $\nu = 0{\cdot}05$. In the strictly deterministic case ($\nu = 0$) the sequence $t_1, t_2, \ldots, t_n$ is determined using the algorithm described in section 2, where the sinusoidal threshold is approximated as a piecewise linear function interpolated at 100 points in one period. With noise, t_i is the sum of two numbers, the deterministic component plus a stochastic component found using a quasi-random number generator (RSTART in Fortran IV).

Figure 2 shows representative firing patterns for the stochastic model with 5% noise. The parameters were chosen to give qualitative agreement with the coupling patterns shown in Fig. 1. In Fig. 2(a) ($k = 0{\cdot}05$, $\lambda^{-1} = 1{\cdot}23$) the firing of the oscillator occurs at successively later phases of the sinusoidal oscillator and for approximately every fifth cycle there is no firing [cf. Fig. 1(a)]. In Fig. 2(a) ($k = 0{\cdot}4$, $\lambda^{-1} = 0{\cdot}72$), the firing occurs at preferred phases of the sinusoidal oscillator. However, whether 1 or 2 firings will occur in any period cannot be predicted [cf. Fig. 1(b)].

One objective of this work is to show how statistical methods can be used to compare quantitative properties of unstable coupling patterns with similar qualitative behaviour. To illustrate these techniques, the transition from the 1/2 to 1/1 patterns of (12) for the dynamics in region A ($k = 0{\cdot}1$) and region B($k = 0{\cdot}4$) was numerically investigated. We show how varying amounts of noise can perturb parameters which can be used to characterize the dynamics. Four complementary quantitative measures of the coupling patterns are considered. Although the simple model proposed in section 2 does not capture the complete complexity of the interaction between the respiratory system and the artificial ventilator, the qualitative (topological) properties of the simple model may in fact be preserved in more realistic mathematical models of the respiratory system (see Discussion). For this

reason, and also to give a focus to the numerical simulation, the results of the numerical simulation are compared with the observed dynamics in the data of Fig. 1. We emphasize that the comparison of the model with experimental data is for illustrative purposes only.

(A) COUPLING RATIO

The ratio R between the frequency of the sinusoidal stimulus and the average firing frequency will be called the *coupling ratio*. For the model, the frequency of the sinusoidal oscillator is equal to one and the coupling ratio is approximated by

$$R = \frac{t_{n+m} - t_n}{m} \tag{13}$$

where the t_i are computed using (12). The coupling ratio was numerically computed using (13) with $n = 25$, $m = 400$ for 50 equally spaced points in the range $0{\cdot}50 \leq \lambda^{-1} \leq 1{\cdot}00$, both for the deterministic case and with 5% noise.

Figure 4(a) shows the coupling ratio vs. λ^{-1} for $k = 0{\cdot}1$. Results are indicated by circles for no noise, and triangles for 5% noise. If the coupling ratio is constant to within 0·03% (or less) over two or more consecutive values of λ^{-1}, the coupling ratio is given by a straight line. From theoretical results in the deterministic case it is known that the coupling ratio should be piecewise constant over finite intervals (Peixoto, 1962; Glass & Mackey, 1979). The numerical simulation shows that the size of these intervals, over

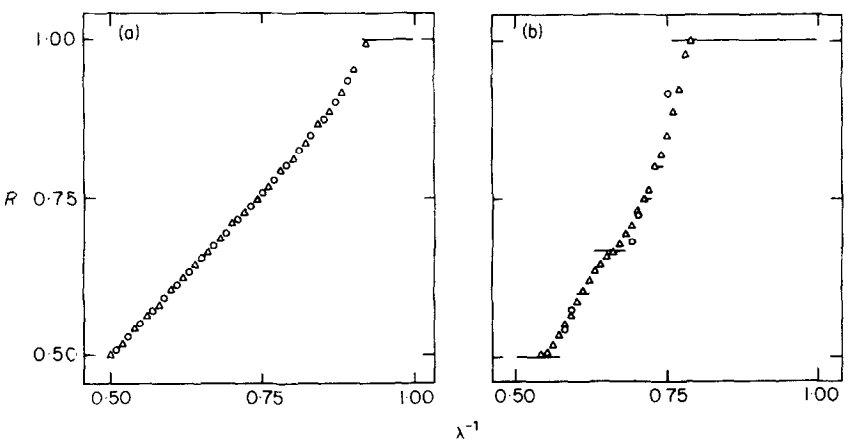

FIG. 4. The coupling ratio R as a function of λ^{-1}. Circles show the case with no noise and triangles the case with 5% noise. (a) $k = 0{\cdot}1$. (b) $k = 0{\cdot}4$.

much of the parameter space, is comparatively small. Using a 50-point grid in the indicated range, only for $0{\cdot}91 \leq \lambda^{-1} \leq 1{\cdot}00$ was a constant coupling ratio over two or more consecutive points found. The coupling ratios with 5% noise are virtually superimposable on those with no noise. Only in the neighbourhood of the transition to the region in which $R = 1$ was there any discrepancy. Thus, for $\lambda^{-1} = 0{\cdot}91$, $R = 0{\cdot}978$ for 5% noise but $R = 1{\cdot}000$ for no noise. For all the points sampled (except for those for which $R = 1$) it was impossible to determine a stable phase locking pattern (see Appendix) and if such patterns did exist they have a very long periodicity.

For $k = 0{\cdot}4$, the situation is very different: for all points sampled with no noise, a stable phase locking pattern could be identified. These results are shown in Fig. 4(b) by the open circles, where a solid horizontal line indicates the cases for which the coupling ratio is constant over two or more consecutive values of λ^{-1}. The preponderance of points sampled displayed "simple" locking patterns. Thus, 46 of the 51 sampled points gave coupling ratios of the form N/M where $N, M \leq 5$ (1/2, 3/5, 2/3, 3/4, 4/5, 1/1). The coupling ratios at the remaining points were 6/11, 4/7, 15/22, 8/11, 10/11. For 5% noise with $k = 0{\cdot}4$ the coupling ratios are shown by triangles. Here the coupling ratios are piecewise constant only over limited ranges, $R = 1/2$ for $0{\cdot}50 \leq \lambda^{-1} \leq 0{\cdot}53$ and $R = 1$ for $0{\cdot}80 \leq \lambda^{-1} \leq 1{\cdot}00$.

The results in Fig. 4 are in qualitative agreement with numerical results found for similar deterministic (Keener, Hoppensteadt & Rinzel, 1980) and stochastic (Moore, Segundo & Perkel, 1963) models.

It is clear that coupling ratios are a very crude measure of the observed dynamics when there is noise. Even though the coupling ratios of a system with and without noise may be identical, the qualitative features of the dynamics in both cases may be very different. To illustrate this, other measures of the observed dynamics are required.

(B) FIRING SEQUENCE

The *firing sequence* is a sequence of non-negative integers which gives the number of firing times of an autonomous oscillator in consecutive cycles of the perturbing oscillator. Thus, the firing sequence $a_1 a_2 \ldots a_n$ represents a coupling pattern in which the autonomous oscillator fires a_i times during the ith cycle of the perturbing oscillator. The firing sequence can be determined from experimental data. For example, the data in Fig. 1(b) are a segment of a record of 50 ventilator cycles in length. The firing sequence for the entire 50 consecutive cycles is

$$\begin{aligned} &1\ 1\ 1\ 1\ 1\ 1\ 2\ 1\ 1\ 2\ 1\ 2\ 1\ 1\ 2\ 1\ 1\ 2\ 1\ 1\ 1\ 2\ 1\ 1\ 2 \\ &1\ 2\ 1\ 1\ 1\ 2\ 1\ 1\ 2\ 1\ 2\ 1\ 2\ 1\ 1\ 1\ 1\ 1\ 1\ 2\ 1\ 1\ 2\ 1\ 2. \end{aligned} \tag{14}$$

The coupling ratio for this sequence is $50/65 = 0{\cdot}770$. In the Appendix a heuristic method is given for determining the firing sequences for stable phase locked patterns of the deterministic model. In this section we give some statistical features of the firing sequence and show how these depend on noise. The case for $k = 0{\cdot}4$ in the neighbourhood of $\lambda^{-1} = 0{\cdot}72$ ($R = 0{\cdot}75$) is examined in detail. For $\lambda^{-1} = 0{\cdot}72$ there is a close correspondence between the statistical features of the firing sequence in the simple model, for certain noise values, and the firing sequence in (14). The technique is appropriate for the firing sequence in (14), and similar methods could be used for other firing sequences.

The firing sequence contains a sparse distribution of twos. To characterize such a firing sequence of length L, let N_1 be the number of times 212 appears, N_2 be the number of times 2112 appears, and so forth. Define

$$n_i = \frac{N_i}{L}, \qquad i = 0, 1, 2, \ldots \tag{15}$$

The values of n_i for (14) are given in Table 1.

TABLE 1

A comparison of the statistical features of the coupling sequence for Fig. 1(*b*), *equation* (14) *and the simple model with* $\lambda^{-1} = 0{\cdot}72$, $k = 0{\cdot}4$ *and* 8% *noise* (*values in parentheses are the s.d.*). *The definition of* n_i *is given in* (15)

	R	n_0	n_1	n_2	n_3
Experiment	0·770	0·000	0·100	0·120	0·040
Simulation	0·765	0·000	0·104	0·111	0·052
	(0·011)	(0·028)	(0·028)	(0·026)	(0·026)
	n_4	n_5	n_6	n_7	n_8
Experiment	0·000	0·000	0·000	0·000	0·000
Simulation	0·024	0·010	0·008	0·001	0·001
	(0·014)	(0·009)	(0·010)	(0·003)	(0·003)

We have computed the values of n_i for the stochastic model for $\lambda^{-1} = 0{\cdot}70$, $0{\cdot}72$, $0{\cdot}74$ and $k = 0{\cdot}4$ at ten noise levels. The computation was performed for 100 consecutive periods of the sinusoidal oscillator starting after a transient of seven periods of the sinusoidal oscillator. Since there is great variability from run to run, the mean and standard deviation, averaged over 10 runs at each parameter value, are given. The values for n_i, $i = 1, 2, 3$, which show large changes as a function of noise and λ^{-1}, are shown in Fig. 5.

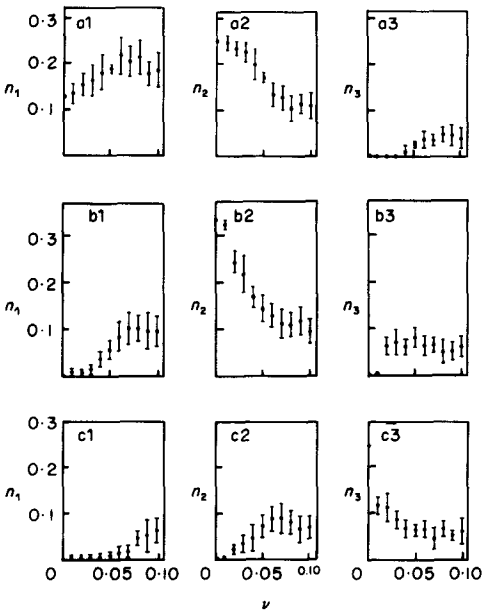

FIG. 5. An analysis of the firing sequences, using n_i defined in (15), as a function of noise in an interval $\pm\nu$. Throughout, $k = 0{\cdot}4$, and $\lambda^{-1} = 0{\cdot}70$ in a1, a2, a3, $\lambda^{-1} = 0{\cdot}72$ in b1, b2, b3, $\lambda^{-1} = 0{\cdot}74$ in c1, c2, c3.

In Table 1 computed values for the model are compared with those observed in (14), and we find good agreement between statistical features of the experimentally observed firing sequence and the model for approximately 8% noise. For comparison, the effects of noise on the model in region A, where $k = 0{\cdot}1$ and $\lambda^{-1} = 0{\cdot}72$, are shown in Fig. 6.

In addition to the coupling ratio and firing sequence other quantitative measures can be used to characterize the nature of the coupling. Two

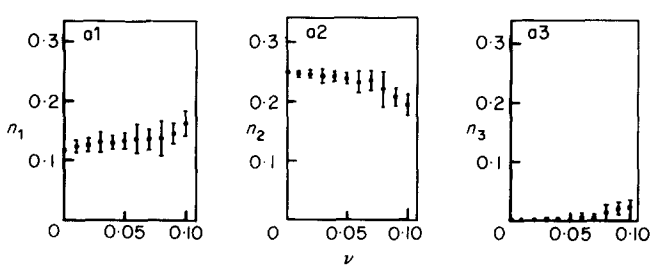

FIG. 6. As in Fig. 5, with $k = 0{\cdot}1$ and $\lambda^{-1} = 0{\cdot}72$.

additional experimentally accessible measures readily derived from a knowledge of the precise firing times are described below.

(C) PHASE DENSITY

In a phase locked deterministic system there are a finite number of values of t_i (mod 1). In stochastic systems, and in deterministic systems which are not phase locked, the number of firing times (mod 1) is infinite.

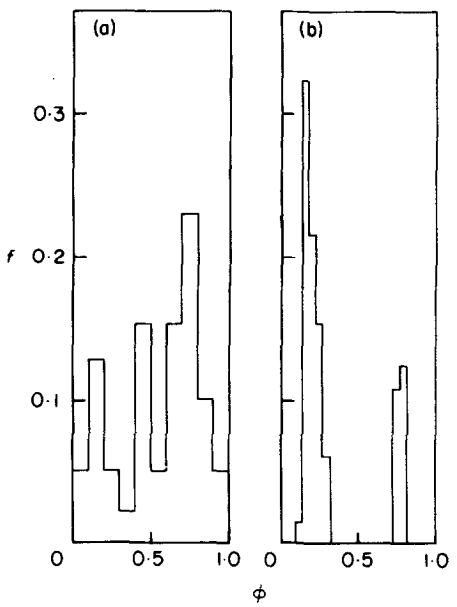

FIG. 7. The phase density histogram for the experimental system averaged over 50 consecutive cycles of the ventilator. Zero phase is taken as the ventilator maximum. (a) The period of the ventilator is 2·0 s and the amplitude is 18 ml [an excerpt is shown in Fig. 1(a)]. (b) The period of the ventilator is 4·2 s and the amplitude is 30 ml [an excerpt is shown in Fig. 1(b)].

In Fig. 7 histograms for the phase of the onset of phrenic firing for the data of Fig. 1 are shown. Similar histograms for the model system at three noise levels, for $\lambda^{-1} = 0{\cdot}72$, are shown in Fig. 8(a) for $k = 0{\cdot}1$ and Fig. 8(b) for $k = 0{\cdot}4$. The histograms are computed over 400 consecutive cycles of the sinusoidal threshold modulation after a transient of 25 cycles. For $k = 0{\cdot}1$ the phase density is continuously distributed over the entire period of the threshold modulation for zero noise. This is the behaviour expected for a quasi-periodic system (with an irrational rotation number) in region A.

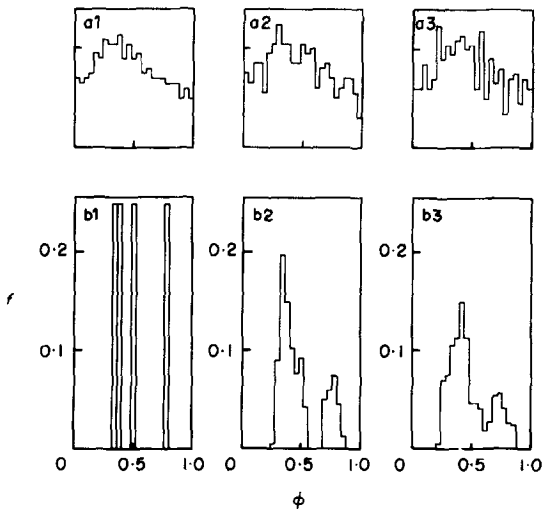

FIG. 8. The phase density histogram for the model system with $\lambda^{-1} = 0{\cdot}72$ at three noise levels, no noise in a1 and b1, 5% noise in a2 and b2, 10% noise in a3 and b3. $k = 0{\cdot}1$ in a and $k = 0{\cdot}4$ in b.

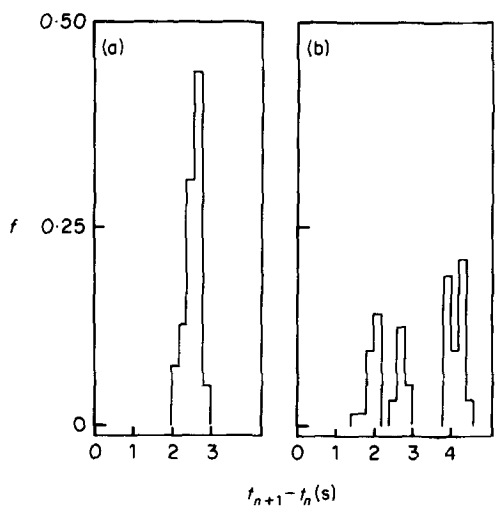

FIG. 9. The relative density of intervals between the onset of successive phrenic activity periods averaged over 50 consecutive cycles of the ventilator. (a) Period of the ventilator is 2·0 s and amplitude is 18 ml [an excerpt is shown in Fig. 1(a)]. (b) Period of the ventilator is 4·2 s and amplitude is 30 ml [an excerpt is shown in Fig. 1(b)].

However, the numerical simulation does not discriminate between this behaviour and a phase locked system with very long periodicity. Noise does not substantially change the histogram of firing density in region A.

For $k = 0{\cdot}4$, $\lambda^{-1} = 0{\cdot}72$, with no noise there is 3/4 phase-locking and firing occurs at four discrete times during the sinusoidal cycle. With noise these peaks become broadened, but with the noise levels used here there remain intervals during the cycle of zero firing density. The experimentally observed firing densities are sharply peaked and the high noise levels needed to find agreement with the firing sequence with $\lambda^{-1} = 0{\cdot}72$ (section 3.B) seem inconsistent with the observed firing density histogram.

(D) INTERSPIKE INTERVAL DENSITY

The interspike interval histogram, which gives the distribution for $t_{n+1} - t_n$ is closely related to the phase density histogram. Figure 9 contains the interspike interval histogram for the data of Fig. 1. The interspike interval histograms for the model with $\lambda^{-1} = 0{\cdot}72$ are given in Fig. 10(a) for $k = 0{\cdot}1$ and Fig. 10(b) for $k = 0{\cdot}4$. For $k = 0{\cdot}1$, the interspike interval histogram is

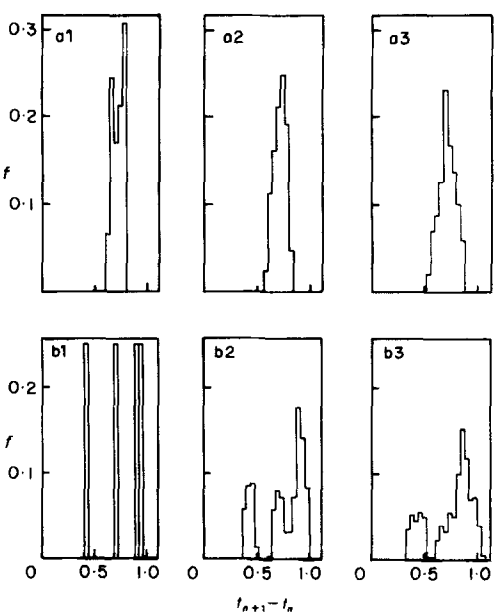

FIG. 10. The interspike interval histogram for the model system $\lambda^{-1} = 0{\cdot}72$ at three noise levels, no noise in a1 and b1, 5% noise in a2 and b2, 10% noise in a3 and b3. $k = 0{\cdot}1$ in a and $k = 0{\cdot}4$ in b.

sharply peaked in the region of the natural period of the oscillator ($t_{n+1} - t_n = 0{\cdot}72$) at all noise levels examined. With noise these peaks become substantially broadened.

4. Discussion

The effects of noise on a simple model for phase locking of biological oscillators have been described. This model has a number of properties which parallel findings in phase locking experiments.

(a) Noise selectively destroys phase locking patterns. As the noise amplitude increases, the number of remaining observable phase locking patterns decreases. This provides one possible explanation for the predominance of simple phase locking patterns (e.g. 2/1, 3/2, 1/1, 2/3, 1/2) in experimental studies.

(b) In the presence of noise, in the regions of phase space between stable phase locking patterns, there are unstable zones in which there is no phase locking. Two qualitatively different types of unstable dynamics, which can be distinguished using the techniques of sections 3.B, 3.C and 3.D, have been found.

  (i) For low amplitude threshold oscillations, the unstable zone is similar to quasi-periodic dynamics. A large number of experimental studies have produced data suggestive of similar dynamics (see Introduction).

  (ii) For high amplitude threshold oscillations, the dynamics in the unstable zone is characterized by stochastic skipped (or intercalated) beats. Similar phenomena are illustrated in the clinical literature on cardiac arrhythmias as well as in the ventilator–respiratory oscillator system.

Although we believe that these two qualitatively different modes of unstable dynamics (which account for most of the unstable patterns observed to date), will be observed in biological phase locking experiments, current published data are inadequate to support this contention. In most of the references cited in the Introduction which deal with unstable coupling behaviour, few data were presented which can be used to sharply characterise the unstable patterns. Many authors seem to regard these unstable patterns as curiosities or annoyances, and have not directed sufficient attention to understanding the mechanism underlying their generation. Study of these unstable patterns may provide a sharp quantitative test of theories for the generation and coupling of biological oscillations, and may also given a new way to characterize stochastic fluctuations in experimental systems.

In the deterministic model (section 2) it has been possible to prove that only two qualitatively different modes of non-phase locked dynamics can be found. The major motivation for the present work was the experimental observation of unstable patterns (Fig. 1) apparently related to these two qualitatively different types of unstable dynamics. We do not know how to rigorously define these two different modes of behaviour, and cannot prove that these are the only two types of unstable behaviour found in the stochastic model (12). In the neighbourhood of the boundary separating regions A and B in Fig. 3, the distinctions between the two different unstable modes in the stochastic system are likely to be blurred. Consequently, it is possible that a single unified mathematical description may account for the statistical features of the two types of unstable dynamics. The mathematical problems involved require further analysis.

The properties of this model seem consistent with experimental observations on phase locking in experimental systems. Reports of other types of qualitative dynamics (e.g. bistability or hysteresis) which cannot be accounted for using our simple model are rare (Moulopoulos, Kardaras & Sideris, 1965). Thus, we are confronted with the problem of understanding how the analysis of coupling phenomena in complex non-linear equations appropriate to model biological oscillations could reduce to, or be equivalent to, the analysis of the simple one dimensional model analyzed here. Any results in this direction would be worthwhile in view of the mathematical difficulty inherent in analyzing the coupling of limit cycle oscillations to periodic driving stimuli (for references see Flaherty & Hoppensteadt, 1978).

There are at least two alternative hypotheses for the generation of irregular patterns, such as those shown in Fig. 1. Many authors have observed that mathematical models for the coupling of a periodic stimulus to a two-dimensional oscillator may show bistability in certain regions or parameter space (Hayashi, 1964; Flaherty & Hoppensteadt, 1978). For example, for some sets of parameter values the time-driven van der Pol oscillator may assume either 1/1 or 1/3 phase-locking patterns, depending on the initial conditions. Since one expects that the basins of attraction of these patterns are complexly intertwined, under the presence of noise, there may be quasi-random skipping between basins of attraction of the different phase-locking patterns, leading to an irregular pattern.

Another possibility is that the experimentally observed irregular locking patterns may correspond to "chaotic" dynamical regions in purely deterministic mathematical models for the interaction of limit cycles with a periodic driving force. Such phenomena have recently been described in the "Brusselator" with a sinusoidal input (Tomita & Kai, 1978). An analogue electrical system of two coupled oscillators has also shown "chaotic"

dynamics (Gollub, Brunner & Danly, 1978). However, the generality and characteristics of the resulting chaotic dynamics are not currently understood.

Unstable and irregular coupling patterns such as those shown in Fig. 1 may be a much more general phenomenon than has been previously recognized. By drawing attention to a possible mechanism to generate these patterns, and showing how they may be classified and characterized, we hope to stimulate work specifically directed towards the analysis of these unstable patterns.

We have benefited from conversations with A. Lasota, J. Gollub and M. Guevara. This research was supported by Grant Z-0091 from the National Science and Engineering Research Council of Canada, and by a studentship (to G.A.P.) from Conseil de la Recherche en Santé du Québec. We thank T. Trippenbach for assistance with the experiments.

REFERENCES

AYERS, J. L. & SELVERSTON, A. I. (1979). *J. Comp. Physiol.* **129,** 5.
BOITEUX, A., GOLDBETER, A. & HESS, B. (1975). *Proc. natn. Acad. Sci. U.S.A.* **72,** 3829.
BRADLEY, G. W., VON EULER, C., MARTTILA, I. & ROOS, B. (1975). *Biol. Cybernetics* **19,** 105.
BROOKS, C. McC. & LU, H.-H. (1972). *The Sinoatrial Pacemaker of the Heart,* ch. 6, Springfield, Illinois: Charles C. Thomas.
BUNNING, E. (1967). *The Physiological Clock.* Berlin: Springer-Verlag.
CLARK, F. J. & VON EULER, C. (1972). *J. Physiol., Lond.* **222,** 267.
CODDINGTON, E. A. & LEVINSON, N. (1955). *Theory of Ordinary Differential Equations.* New York: McGraw-Hill.
COHEN, M. I. & FELDMAN, J. L. (1977). *Federation Proc.* **36,** 2367.
FLAHERTY, J. &. HOPPENSTEADT, F. C. (1978). *Studies in appl. Math.* **58,** 5.
GLASS, L. & MACKEY, M. C. (1979). *J. math. Biol.* **7,** 339.
GOLLUB, J., BRUNNER, T. O. & DANLY, B. G. (1978). *Science* **200,** 48.
HARDY, G. H. & WRIGHT, E. M. (1960). *An Introduction to the Theory of Numbers,* 4th Edn. Oxford: Clarendon Press.
HAYASHI, C. (1964). *Nonlinear Oscillations in Physical Systems.* New York: McGraw-Hill.
HERMAN, M. R. (1977). In *Lecture Notes in Mathematics no. 597, Geometry and Topology,* p. 271. Berlin: Springer-Verlag.
KEENER, J. P. (1980). *Trans. Am. Math. Soc.* (in press).
KEENER, J. P., HOPPENSTEADT, F. C. & RINZEL, J. (1980). *SIAM J. Appl. Math.,* in press.
MOORE, G. P., SEGUNDO, J. P. & PERKEL, D. H. (1963). In *Proceedings of the San Diego Symposium for Biomedical Engineering* (A. Paull, ed.). La Jolla, California: San Diego Symposium for Biomedical Engineering.
MOSER, J. (1973). *Stable and Random Motions in Dynamical Systems.* Princeton, N.J.: Princeton University Press.
MOULOPOULOS, S. D., KARDARAS, N. & SIDERIS, D. A. (1965). *Am. J. Physiol.* **208,** 154.
NAGUMO, J. & SATO, S. (1972). *Kybernetik* **10,** 155.
PAVLIDIS, T. (1973). *Biological Oscillators: Their Mathematical Analysis,* ch. 4. New York: Academic Press.
PEIXOTO, M. M. (1962). *Topology* **1,** 101.

PERKEL, D. H., SCHULMAN, J. H., BULLOCK, T. H., MOORE, G. P. & SEGUNDO, J. P. (1964). *Science* **145,** 61.
PETRILLO, G. A., GLASS, L. & TRIPPENBACH, T. (1980). In preparation.
PICK, A., LANGENDORF, R. & JEDLICKA, J. (1973). In *Complex Electrocardiography 1* (C. Fisch, ed.), p. 113. Philadelphia: F. A. Davis.
PILKINGTON, J. B. (1976). *Experientia* **32,** 1435.
PINSKER, H. M. (1977). *J. Neurophysiol.* **40,** 544.
REID, J. V. O. (1969). *Am. Heart J.* **78,** 58.
SATO, S. (1972). *Kybernetik* **11,** 208.
STEIN, P. S. G. (1976). In *Neural Control of Locomotion* (R. M. Herman, S. Grillner, P. S. G. Stein & D. G. Stuart, eds), p. 465. New York: Plenum.
STEIN, P. S. G. (1978). *J. Comp. Physiol.* **124,** 203.
SWADE, R. H. (1969). *J. theor. Biol.* **24,** 227.
TOMITA, K. & KAI, T. (1978). *Prog. Theor. Phys. Supp.* **64,** 280.
VAN DER TWEEL, L. H., MEIJLER, F. L. & VAN CAPELLE, F. J. L. (1973). *J. appl. Physiol.* **34,** 283.
VON HOLST, E. (1973). *The Behavioural Physiology of Animals and Men.* London: Methuen.
WATANABE, Y. & DREIFUS, L. S. (1977). *Cardiac Arrhythmias: Electrophysiologic Basis for Clinical Interpretation.* New York: Grune & Stratton.
WENDLER, G. (1974). *J. comp. Physiol.* **88,** 173.
WILKENS, J. L. & YOUNG, R. E. (1975). *J. exp. Biol.* **63,** 219.
WYMAN, R. J. (1977). *Ann. Rev. Physiol.* **39,** 417.

APPENDIX

The Firing Sequence

For the stochastic model the criterion for phase locking given in (9) is no longer applicable since t_n has a random component equation (12). A useful method for analyzing the dynamics in this case is the firing sequence, defined as follows. For each period of the sinusoidal oscillator, count the number of times the oscillator reaches threshold. The resulting sequence of integers is the firing sequence. For the stochastic system we use periodicity of the firing sequence as a criterion for phase locking (section 3.A). For example, the firing sequence for 1/2 phase locking is ...222... and for 1/1 phase locking is ...111.... These firing sequences are observed even with 5% noise with $k = 0{\cdot}4$.

We have developed a method to determine the firing sequences for the deterministic mathematical model of phase locking presented in section 2. The method is heuristic and has been checked on a large number of phase locked patterns observed here and previously (Glass & Mackey, 1979). Another algorithm, essentially identical to ours, has been given to compute firing patterns of a model neuron under constant input (Nagumo & Sato, 1972; Sato, 1972). Although the physical interpretation of this earlier work is different from ours, the mathematical model is topologically equivalent to the model in section 2 in region B of (λ, k) phase space. The model in

Nagumo & Sato (1972) is piecewise linear, and consequently it is amenable to analytical computations. Thus, although we have not proven the validity of the algorithm, a proof of its validity for a topologically equivalent model is available (Nagumo & Sato, 1972; Sato, 1972).

We first describe a method for generating rational fractions (Hardy & Wright, 1960; Sato, 1972; Keener, 1980). Consider two non-negative rational fractions h/k and h'/k' in the interval [0, 1] (the rational fraction 0/1 corresponds to the integer 0). The *mediant* of these two fractions is defined $(h+h')/(k+k')$, where $h/k<(h+h')/(k+k')<h'/k'$. By successively computing mediants between any two starting fractions, all intermediate rational fractions are generated. This is illustrated by the construction in Table 2(a). Starting from the "seed values" 1/2 and 1/1 in line 1, each successive line contains the mediants plus the entries of the preceding line. The nth line contains $2^{n-1}+1$ entries. The resulting sequences, reading from left to right, share many properties with the Farey series (Hardy & Wright, 1960).

TABLE 2

(a) *Rational numbers*								
1/2								1/1
1/2				2/3				1/1
1/2		3/5		2/3		3/4		1/1
1/2	4/7	3/5	5/8	2/3	5/7	3/4	4/5	1/1
(b) *Repeating units of firing sequences for coupling ratios between* 1/2 *and* 1/1								
2								1
2				21				1
2		221		21		211		1
2	2221	221	22121	21	21211	211	2111	1

Firing sequences for the deterministic system are found in a similar fashion. The firing sequences for a phase locked pattern is a periodic sequence of integers $\ldots a_1a_2\ldots a_ja_1\ldots a_j\ldots$ where each a_i is an integer and the sequence $a_1a_2\ldots a_j$ is called the *repeating unit.* By definition, if there is N/M phase locking then

$$j=N, \qquad \sum_{i=1}^{j} a_i = M. \tag{A1}$$

Consider two firing sequences, one with a repeating unit $a_1a_2\ldots a_j$ and the other with a repeating unit $b_1b_2\ldots b_k$. The *ordered sum* of the repeating units is defined as the sequence $a_1a_2\ldots a_jb_1b_2\ldots b_k$. If the sequence $a_1a_2\ldots a_j$

corresponds to a coupling ratio of N/M and $b_1 b_2 \ldots b_k$ corresponds to a coupling ratio of N'/M' then from (A1) and the definition of the firing sequence, the ordered sum corresponds to the locking ratio $(N+N')/(M+M')$, i.e. the mediant of the two initial coupling ratios.

The firing sequences observed for the different locking patterns in the deterministic system can be computed by computing the ordered sum of the repeating units provided the appropriate seed values for the initial repeating units are used. These are given in Table 3. The repeating unit for any locking

TABLE 3

The seed values used to compute repeating units for different coupling ratios

Coupling ratio	1/4	1/3	1/2	1/1	2/1	3/1	4/1
Repeating unit	4	3	2	1	10	100	1000

ratio is determined as illustrated in Table 2(b), which gives the repeating units for the coupling ratios lying between 1/2 and 1/1. Starting from the seed values 2 and 1 in line 1, each successive line contains the ordered sums plus the entries in the preceding line. From (A1) there is a one-to-one correspondence between the entries in Tables 2(a) and 2(b). Note that the firing sequence in (14) is consistent with a phase locking pattern 38/50. Using the methods in this section, the repeating unit for this ratio would be 2112112112112112111 which is very different from that which was observed. Starting from appropriate seed values, the repeating units for other coupling ratios can be computed.